

Magnetic Eigenmaps for Visualization of Directed Networks

Michaël Fanuel ^{*}, Ángela Fernández [†], Carlos M. Alaíz [‡] and Johan A. K. Suykens [§]

KU Leuven, ESAT, STADIUS Center. B-3001 Leuven, Belgium.

October 12, 2021

We propose a framework for visualization of directed networks relying on the eigenfunctions of the magnetic Laplacian, called here Magnetic Eigenmaps. The magnetic Laplacian is a complex deformation of the well-known combinatorial Laplacian. Features such as density of links and directionality patterns are revealed by plotting the phases of the first magnetic eigenvectors. Directed networks being common in social science, biology or computer science, our visualization method may be relevant for the field of complex networks, as well as applied mathematics and machine learning. Illustrations of our method are given for both artificial and real-life networks.

1 Introduction

Many objects and problems in neuroscience, biology, social or computer science are phrased in terms of networks and graphs. The embedding of data points forming undirected graphs can be performed using manifold learning methods, among which we can underline the so-called Laplacian Eigenmaps [1], or Diffusion Maps [2]. In the same spirit, the embedding of a directed graph originated from the sampling of a vector field on a manifold was studied in [3]. A Laplacian for strongly connected and aperiodic directed networks was introduced by Chung [4] in relation with a random walk process, which was used for visualization for instance in [5]. Actually, Laplacians are very useful tools for community detection and data visualization. A common feature of these approaches is the relevance of the discrete or combinatorial Laplacian, and its normalized versions.

In this paper, no assumption on the origin of directed networks is needed, so we could deal, for example, with networks of webpages which are not embedded in any vector space. In particular, we propose here the use of another Laplacian which naturally exists for a general connected directed network, called the magnetic Laplacian. Known in the physics literature, it is actually a vector bundle Laplacian as described by Kenyon [6, 7]. The method that we describe assigns a complex rotation, i.e., an element of $U(1)$, to each directed link, and the orientation of the link determines the direction of the rotation.

2 Magnetic Laplacian and Eigenmaps

Laplacian Eigenmaps have been designed for embedding undirected graphs and for dimensionality reduction of data. Given a symmetric weight matrix $W^{(s)} = \{w_{ij}^{(s)}\}$, the maps are associated to the eigenvectors of the combinatorial Laplacian $L^{(0)} = D - W^{(s)}$ where D is the diagonal degree matrix whose elements are given by the sum of each row of the weight matrix.

In the case of directed networks, the graphs are given by an unsymmetric weight matrix, $W = \{w_{ij}\}$. For simplicity, we suppose that the weights are binary, i.e. $w_{ij} = 1$ if there is a link from i to j and $w_{ij} = 0$ otherwise. The weight matrix W can be decomposed as a symmetric term $w_{ij}^{(s)} = (w_{ij} + w_{ji})/2$, that indicates the existence of a connection between i and j , and a skew-symmetric term, the edge flow $a_{ij} = -a_{ji}$, that encodes the direction of the link, so that $a_{ij} = 1$ if the link points from i to j .

In this context, the Magnetic Laplacian can be defined as $L^{(g)} = D - T^{(g)} \odot W^{(s)}$, where D is the degree matrix associated to the symmetrized weight matrix, $0 \leq g < 1/2$ is an electric charge parameter that quantifies the importance of the directional information, and $T^{(g)} \odot W^{(s)} = \{\exp(i2\pi g a_{ji}) w_{ij}^{(s)}\}$ (notice the Hadamard product \odot).

The eigenfunctions $\phi_k^{(g)}$ of the magnetic Laplacian, namely *Magnetic Eigenmaps* [8], provide a map of the nodes in \mathbb{C}^n . They satisfy the optimality criterion of the minimization of

$$\sum_{i,j} w_{ij}^{(s)} \left| f_i - e^{i2\pi g a_{ji}} f_j \right|^2 \quad (1)$$

over the complex functions of the nodes f of unitary norm, so that the eigenfunction of smallest eigenvalue of $L^{(g)}$, $\phi_0^{(g)}$, is the minimizer of (1).

The magnetic Laplacian, already known in the physics community [9, 10, 11], is in fact a connection Laplacian [6], as studied by Singer and Wu [12], except that here we associate to each link an element of the complex rotation group $U(1)$, instead of an orthogonal matrix of $SO(d)$. Its spectrum is real and positive semi-definite. Actually, as we have said before, the magnetic Laplacian depends also on a parameter g , interpreted as an electric charge, which adds some extra flexibility in the visualization process. More explicitly, in general, we propose to choose a quantized charge $g = k/m$ with $k \notin m\mathbb{Z}$. The particular value $g = 1/3$ is suited in the presence of directed triangles, while $g = 1/4$ is relevant in the presence of directed 4-cycles. We observe empirically that $g = 2/5$ gives also good results in the presence of reciprocal links. For more details we refer to [8]. Notice that choosing $g > 1/2$ would be equivalent to a flip of all link directions.

Interestingly, the magnetic Laplacian can be interpreted as a discrete quantum mechanical Hamiltonian of a charged particle on a network, influenced by a magnetic flux. The objective function of (1) is the corresponding energy of the wave function f . Similarly, the combinatorial Laplacian is a discrete Hamiltonian of a free particle on a network.

3 Visualization of density and directionality

Going into detail in the relation between the combinatorial and the magnetic Laplacians, in the case when the edge flow

^{*}Email: michael.fanuel@esat.kuleuven.be.

[†]Email: angela.fernandez@esat.kuleuven.be.

[‡]Email: cmalaiz@esat.kuleuven.be.

[§]Email: johan.suykens@esat.kuleuven.be.

of the network is given exactly by a certain potential h , i.e. $a_{ij} = h_j - h_i$ for any nodes i and j , then the spectrum of the magnetic Laplacian corresponds to the spectrum of the combinatorial Laplacian, and the eigenvectors are related by $\phi_{k,i}^{(g)} = e^{i2\pi g h_i} \phi_{k,i}^{(0)}$.

Such a particular case can be characterized by the first eigenvalue, as stated in the following theorem.

Theorem 1. *Let us considered a connected graph. The magnetic Laplacian $L^{(g)}$ has a zero eigenvalue iff there exists a function h satisfying, for any link $\{i, j\}$, $a_{ij} = h_j - h_i$.*

Proof. Both implications are proved next:

\Rightarrow If $L^{(g)}$ has a zero eigenvalue, we know that the Rayleigh quotient for $\phi_0^{(g)}$ is

$$\sum_{i,j} w_{ij}^{(s)} \left| \phi_{0,i}^{(g)} - e^{i2\pi g a_{ji}} \phi_{0,j}^{(g)} \right|^2 = 0,$$

and therefore, each term in this finite sum has to vanish. Hence, for any link $\{i, j\}$, we have $\phi_{0,i}^{(g)} = e^{i2\pi g a_{ji}} \phi_{0,j}^{(g)}$, so that the eigenfunction has a constant modulus $|\phi_{0,i}^{(g)}| = c$. Indeed, it can be decomposed as $\phi_{0,i}^{(g)} = c \cdot e^{i\theta_i}$. Consequently, for any link $\{i, j\}$, $e^{i2\pi g a_{ji}} = e^{i(\theta_i - \theta_j)}$, and therefore, $2\pi g a_{ji} = \theta_i - \theta_j + 2\pi m$, with m an integer. Because $a_{ji} = -a_{ij}$ by definition, we find that $m = 0$. Hence, we choose $h_i = \theta_i / (2\pi g)$.

\Leftarrow If, for any link $\{i, j\}$, we have $a_{ij} = h_j - h_i$, then we can write $L^{(g)} = U^{-1} L^{(0)} U$, with the unitary diagonal matrix U of matrix elements $U_{ii} = e^{i2\pi g h_i}$, and where $L^{(0)} = D - W^{(s)}$ is the combinatorial Laplacian. \square

This property may be also understood as a consequence of the results of [11, 10] in the context of mathematical physics. Therefore, the function h , interpreted as a potential responsible for the link directions [13], is effectively encoded in the phase of the eigenvectors, up to a constant shift. In the ranking context, h is called a consistent ranking. In practice, obtaining h requires to solve a linear system or to calculate the pseudo-inverse of the combinatorial Laplacian as explained in the combinatorial Hodge theory of [13]. Incidentally, the magnetic Laplacian has interesting relations to the topology of graphs [10, 11].

In order to introduce now our method, we consider first this previous particular type of directed networks. Let us further assume that the symmetrized weight matrix $W^{(s)}$ is associated to a connected undirected graph with a clear cluster structure. Hence, we have in general that the first eigenvector of the combinatorial Laplacian is constant, $\phi_{0,i}^{(0)} = \text{cst}$, whereas the sign of the so-called Fiedler vector, $\text{sign}(\phi_{1,i}^{(0)})$, partitions the network in two dense subgraphs. If a clear cluster structure is present, then the “phase” of the Fiedler eigenvector is piecewise constant on the clusters. Therefore, it is interesting to calculate the complex phase of the first eigenvector of the magnetic Laplacian, i.e. $\text{phase}(\phi_{0,i}^{(g)}) = 2\pi g h_i \bmod 2\pi$, which gives the potential h . Furthermore, the phase of the second magnetic eigenvector $\phi_{1,i}^{(g)}$ is exactly equal to the phase of the first magnetic eigenvector $\phi_{0,i}^{(g)}$, but shifted by π on the nodes where the Fiedler eigenvector is negative, $\text{sign}(\phi_{1,i}^{(0)}) = -1$. To summarize, in this perfect case: (i) $\text{phase}(\phi_{0,i}^{(g)})$ incorporates the directionality information (corresponding to h); and (ii) $\text{phase}(\phi_{1,i}^{(g)})$ incorporates the density information (corresponding to the spectral clustering).

In practice, the edge flow does not satisfy the condition $a_{ij} = h_j - h_i$, and thus the explanation given above is only an

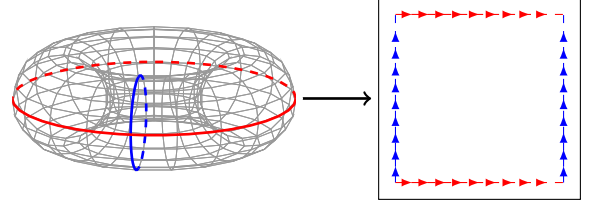


Figure 1: Identification of the 2-torus with the square $[0, 2\pi] \times [0, 2\pi]$ with identified sides. Notice that the position of the cuts is arbitrary, and it can be adapted to each particular dataset for the sake of clarity.

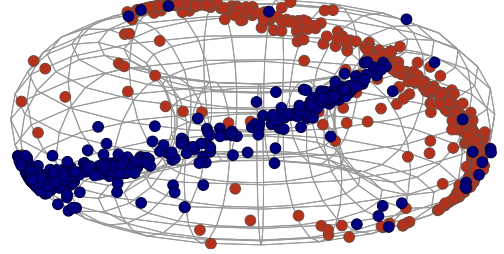


Figure 2: Example of the magnetic eigenmaps plotted over the 3-dimensional 2-torus for a graph with two communities, corresponding to the dataset “Political Blogosphere” explained in detail in the applications section.

approximation. Actually, due to the inhomogeneous degree distribution of real-life networks it can be advantageous to normalize the magnetic Laplacian as follows $L_N^{(g)} = D^{-1/2} L^{(g)} D^{-1/2}$, so that we only have to compute the largest eigenvalues of $D^{-1/2} T^{(g)} \odot W^{(s)} D^{-1/2}$. Once the Laplacian is normalized, we propose to embed the network by the following mapping

$$i \mapsto \left(\text{phase}(\phi_{0,i}^{(g)}) \quad \text{phase}(\phi_{1,i}^{(g)}) \quad \dots \quad \text{phase}(\phi_{n,i}^{(g)}) \right)^T.$$

Notice that the phase operator identifies the angles that differs by 2π , which means that the geometrical representation, for the 1-dimensional case, is just a circle, whereas for the general n -dimensional case is an n -torus. Hence, for visualization purposes, the directed network will be embedded on a 2-torus represented as the square $[0, 2\pi] \times [0, 2\pi]$ with opposite sides identified, as shown in Figures 1 and 2. Therefore, the visualization will be symmetric if an eigenvector undergoes a global rotation in the complex plane (note that given an eigenvector $\phi_k^{(g)}$ of the magnetic Laplacian, another eigenvector of the same eigenvalue is given by $e^{i\alpha} \phi_k^{(g)}$). We will show empirically that this low dimensional embedding is able to visualize at the same time dense regions of links, revealed by the y -axis, and patterns determined by the link directions, given by the x -axis.

4 Connection with Vector Diffusion Maps

The computation of the eigenvectors of the normalized magnetic Laplacian can resemble the Vector Diffusion Maps of Singer and Wu [12], although in our case we work with a complex and unitary transporter in $U(1)$, instead of with an orthogonal transporter. For the sake of completeness, let us outline the relationship between Magnetic Eigenmaps and Vector Diffusion Maps.

Vector Diffusion Maps describes the transport of a vector v_j from the tangent space at point j to the tangent space at i through an orthogonal transformation O_{ji} , followed by an

Algorithm 1 Magnetic Eigenmaps Visualization

procedure MEIGENMAPS(W, g)*Magnetic Laplacian.*

$$W^{(s)} \leftarrow (W + W^\top) / 2 \quad \triangleright \text{Symmetric weights.}$$

$$A \leftarrow W - W^\top \quad \triangleright \text{Edge flow.}$$

$$d_{ii} \leftarrow \sum_j w_{ij}^{(s)} \quad \triangleright \text{Degree matrix.}$$

$$t_{ij}^{(g)} \leftarrow e^{i2\pi g a_{ji}} \quad \triangleright \text{Transporter.}$$

$$L^{(g)} \leftarrow D - W^{(s)} \odot T^{(g)} \quad \triangleright \text{Magnetic Laplacian.}$$

Normalization.

$$L_N^{(g)} \leftarrow D^{-1/2} L^{(g)} D^{-1/2} \quad \triangleright \text{Normalized Laplacian.}$$

Eigendecomposition.

$$\phi_0^{(g)}, \phi_1^{(g)}, \dots \leftarrow \text{EIGS}(L_N^{(g)}) \quad \triangleright \text{Eigenvectors.}$$

Mapping.

$$\text{return } \left\{ \text{phase}(\phi_m^{(g)}) \right\}_{m=0}^n \quad \triangleright \text{Phases.}$$

end procedure

averaging process over all possible j 's:

$$(A_{\text{VDM}}v)_i = \frac{1}{d_i} \sum_j w_{ji}^{(s)} O_{ji} v_j. \quad (2)$$

Similarly, for the Magnetic Eigenmaps the transition matrix $A_{\text{ME}} = D^{-1} T^{(g)} \odot W^{(s)}$ describes the transport of a complex number f_j along a link between j to i , followed by an averaging process over all possible j 's connecting i , i.e.

$$(A_{\text{ME}}f)_i = \frac{1}{d_i} \sum_j w_{ji}^{(s)} t_{ji}^{(g)} f_j. \quad (3)$$

Comparing (2) and (3), the main difference, apart from the working space (\mathbb{R}^n and \mathbb{C} , respectively), resides in the transport term. In the case of Vector Diffusion Maps, it is an element of $\text{SO}(n)$ determined by Local PCA, and for Magnetic Eigenmaps it is an element of $\text{U}(1)$ which can be tuned by the user through the parameter g in order to highlight certain properties of the graph. Moreover, the methodology of both approaches differs in the way they map the data. On the one hand, Vector Diffusion Maps follows a natural extension of Diffusion Maps [2], so that each point is mapped to a matrix defined in terms of the eigenvalues and eigenvectors of the transition matrix. On the other hand, the proposed magnetic eigenmaps map the points to the phases of the first eigenvectors of the corresponding Laplacian.

Therefore, although both methods share some similarities, they are essentially different, and none of them can be seen as a particular case of the other.

5 Applications

In what follows, we will illustrate how Magnetic Eigenmaps can be successfully applied to the visualization of directed graphs over two synthetic examples, and two real-world networks. For completeness, we include the procedure to compute the magnetic eigenmaps for a directed graph, given by the binary weights W , in Algorithm 1.

In all the examples we will first depict the aspect of the original network as a baseline, using for this purpose expert knowledge or a force-directed layout, which is just a way of depicting graphs using attractive forces between adjacent nodes and repulsive forces between distant nodes. We will also compare Magnetic Eigenmaps with Diffusion Maps for the real-world examples. In this context, the Diffusion Maps embedding is obtained by computing the algorithm with $g = 0$, and plotting the first eigenvectors of the corresponding Laplacian (instead of their phases). For the real networks we will also depict the eigenvalues decay. According to Theorem 1, the case

$a_{ij} = h_j - h_i$ implies a first eigenvalue equal to 0, so in the cases where the first eigenvalue is near to zero we can interpret the phases of the first pair of eigenfunctions as a representation of the directionality and the density of the graph.

5.1 Artificial networks

We propose to visualize first the artificial network with a running flow of Figure 3a, where the coordinates of the nodes in the real plane have been chosen according to our knowledge about the underlying groups. This network, constructed according to [14], is constituted of three groups of ten nodes (A , B and C). Two nodes in the same group are linked with a probability 0.5. Any node has also a probability 0.5 to be connected to a node from another group. Furthermore 90 percent of these interconnections are directed in the direction of the flow, i.e. $A \rightarrow B$, $B \rightarrow C$ and $C \rightarrow A$. Plotting the real and imaginary parts of the first eigenvector of the magnetic Laplacian can indicate the presence of a running flow in the network, as illustrated in Figure 3b. However there could be also dense clusters in the network which cannot be visualized only thanks to the phase of the first eigenfunction. In order to actually visualize the 3 groups and the density information, we use our proposal of plotting the complex phase of the first eigenfunction versus the phase of the second eigenfunction of the magnetic Laplacian, as illustrated in Figure 3c. Notice that the phase of the second eigenfunction does not distinguish specific dense clusters in the network, while the phase of the first eigenfunction (corresponding to directionality) is able to separate the three groups. This is actually true because the network was constructed in that way.

We are going to consider now an example of network with a small number of nodes playing a particular role and then a clear structure with two dense clusters. In the paper of Leicht and Newman [15], an artificial network of 32 nodes is built as follows: it consists of two dense groups of 14 nodes with a few interconnecting links and two pairs of nodes are connected to the whole network. The first pair has only in-coming links, while the second pair has only out-going links. An illustration using the force layout is given in Figure 4a. Plotting the real and imaginary parts of the first eigenfunction allows to distinguish the two pairs from the rest of the network, as showed in Figure 4b. However, it is more instructive to visualize the network using the phase of the two first eigenfunctions of the magnetic Laplacian. Indeed, the two groups and the two pairs are easily separated in Figure 4c, where the phase of the first eigenfunction (directionality) is able to separate the two pairs of disconnected points from the rest of the set, defining three directionality-groups: green points, the yellow points and the blue and red points together. On the other side, the phase of the second eigenfunction (corresponding to density information) shows two groups: the blue and green points versus the red and yellow points. Combining the information given by the two phases we are able to easily separate visually the four groups that we were looking for.

5.2 Real-life networks

In the previous section, we considered directed networks having known structures either in terms of link directions or link density. Indeed, Magnetic Eigenmaps is able to provide simultaneously information about direction and density, as we illustrate now also on real-life directed networks where these two aspects are relevant.

The first data set used represents the network of *common adjective and noun adjacencies* for the novel “David Copperfield” by Charles Dickens, as described by M. Newman [16]. In

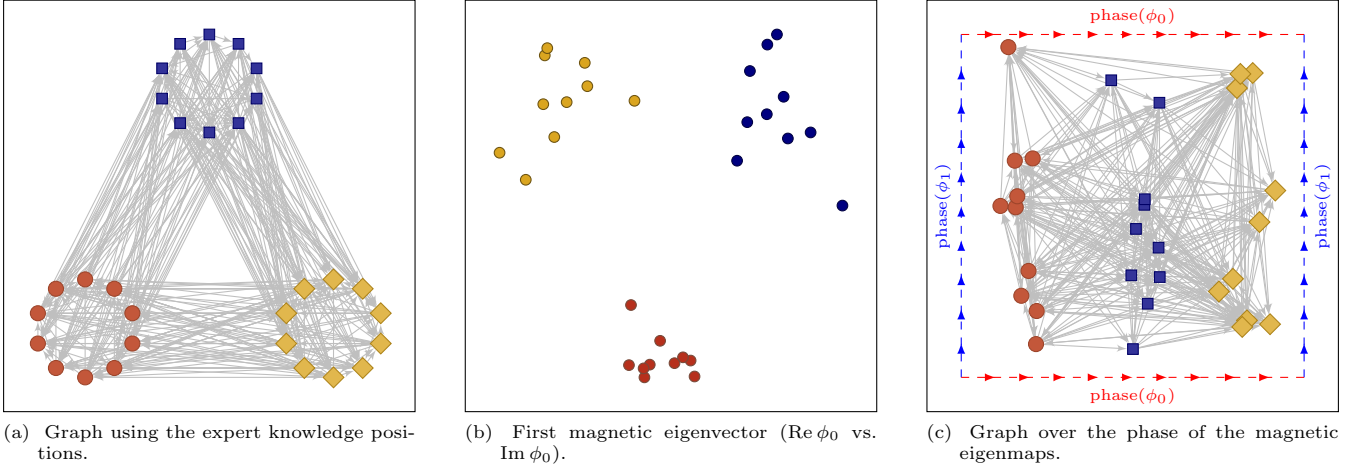


Figure 3: Artificial network with a running flow. The colours indicate the three groups, and the magnetic eigenmaps correspond to $g = 1/4$. Figure 3c is shown over the 3-dimensional torus in the SI appendix.

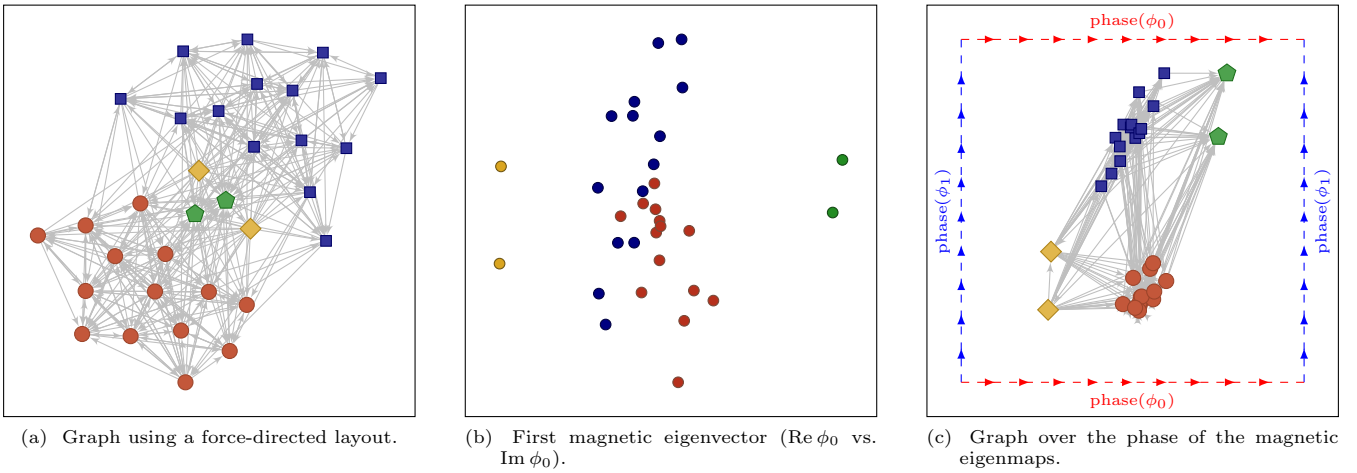


Figure 4: Artificial network with two dense clusters and two pairs of nodes with a specific role. The colours indicate the dense clusters and the hub pairs, and the magnetic eigenmaps correspond to $g = 1/4$. Figure 4c is shown over the 3-dimensional torus in the SI appendix.

this directed graph we have 112 nodes, that represent the most commonly occurring adjectives and nouns in the book. Edges connect any pair of words that occur in adjacent position in the text of the book. From the structure of English, a certain directional structure can be anticipated, i.e. adjectives are expected to be found before nouns. The graph representation of this dataset, using a force layout, is shown in Figure 5a, where the structure can hardly be guessed. However, considering the phase of the two first magnetic eigenmaps, it is possible to visualize the presence of two groups in the directed network, as illustrated in Figure 5b (indeed, the information is provided mostly by the first coordinate, corresponding to directionality). Finally, for comparison purposes we show in Figure 5c the first embedding coordinates in the Diffusion Maps case, more concretely the second and third eigenvectors (the first one is discarded because it is constant). In this case both classes appeared mixed, so these two diffusion coordinates are not able to reveal the structure of the data. The reason is that Diffusion Maps captures the density of the links but not the directionality, while Magnetic Eigenmaps relates both.

In Figure 6 are represented the first eigenvalues of the combinatorial Laplacian ($g = 0$) and the magnetic Laplacian ($g = 2/5$). The increase of these eigenvalues is very contin-

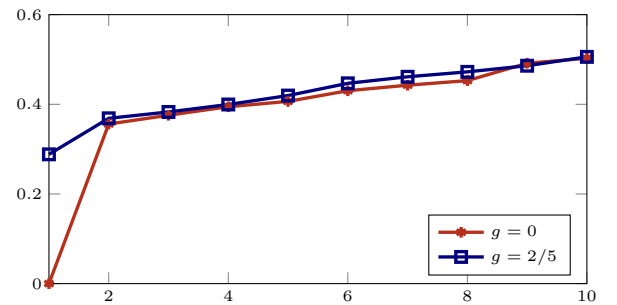


Figure 6: First eigenvalues of the combinatorial ($g = 0$) and magnetic ($g = 2/5$) Laplacians, in the case of the Word Adjacencies network.

uous and homogeneous, presenting just an eigengap between the first eigenvalue and the second one. This result reinforces the election of the first and second eigenvectors for this example as visualization coordinates. Moreover, the differences between the two spectra, and the nonzero initial eigenvalue, show that the structure of the graph is not trivial (see Theorem 1).

The second real dataset used in these experiments represents

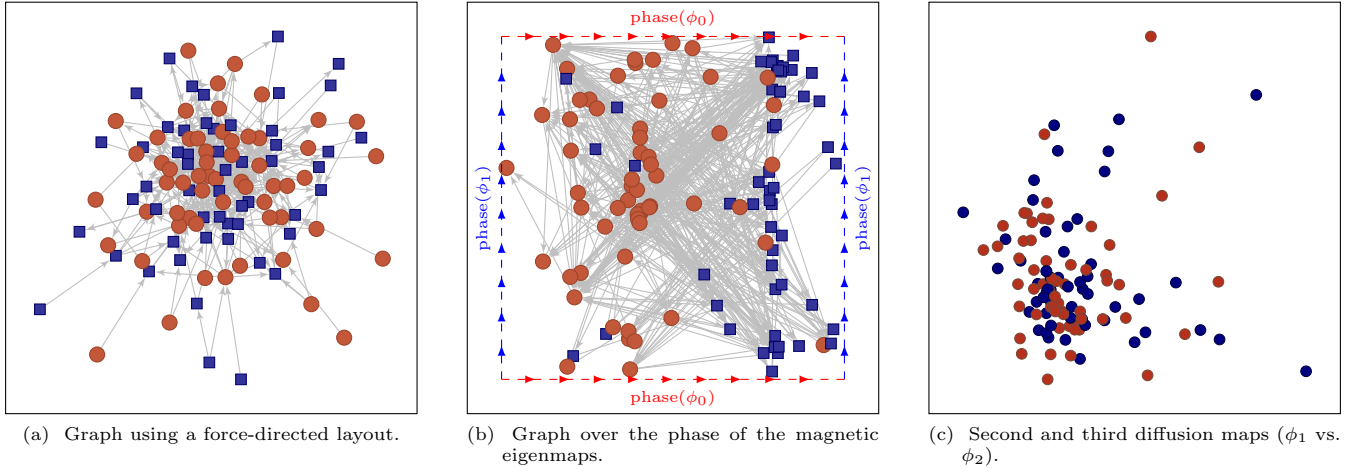


Figure 5: Word adjacencies example. The colours indicate the class labels: nouns (\bullet) and the adjectives (\blacksquare), and the magnetic eigenmaps correspond to $g = 2/5$. Figure 5b is shown in more detailed and also over the 3-dimensional torus in the SI appendix.

the *political blogosphere* in February of 2005, as compiled by Lada Adamic and Natalie Glance [17]. This directed graph is composed by 1222 nodes that indicate the political leaning, meaning left or liberal and right or conservative. We have removed from these data disconnected points. The data on political leaning comes from blog directories and some of the blogs were labelled manually, based on incoming and outgoing links and posts around the time of the 2004 presidential election in the USA. The links between blogs were automatically extracted from a crawl of the front page of the blog. From Figure 7a, where the network has been depicted using the force layout, it is already possible to guess the presence of two dense groups of webpages. The first eigenvalues of the magnetic Laplacian in Figure 8 instruct us to consider the two first pairs of eigenvalues in order to visualize two different structures. In Figure 7b, the magnetic eigenmaps do not distinguish the two classes of nodes, however we observe that some webpages are less connected to the rest of the network, whereas in Figure 7c we see the two classes clearly separated. The latter mapping is also shown in \mathbb{R}^3 over the torus as an illustration in Figure 2. For comparison purposes, we show also in this case the first embedding diffusion coordinates in Figures 7d and 7e. In this example, where the graph structure is clearer than in the previous dataset, Diffusion Maps is able to condense the two classes separately just using the density of the graph. We would like to highlight that the distinction between both classes is not very clear when we select the second and third eigenvectors (the first eigenvector is again discarded), whereas a cleaner classification structure is obtained when the fourth and fifth eigenvectors are depicted. Nevertheless, Magnetic Eigenmaps represents better and in a neat way the connectivity and density structure.

6 Summary and Discussion

In this paper, we have proposed the use of the eigenvectors of the magnetic Laplacian, called here *Magnetic Eigenmaps*, for the visualization of directed networks. Our work is a natural extension of the Laplacian Eigenmaps and it is the first application of a vector bundle Laplacian in the field of complex network. Computationally, the method reduces to the calculation of the eigenvectors of maximal eigenvalues of a Hermitian matrix, which can be conveniently performed thanks to e.g. the power method. The advantages of this approach were explained on artificial and real-life datasets, showing that our method is

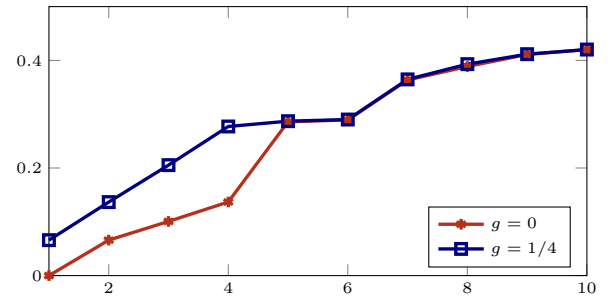


Figure 8: First eigenvalues of the normalized magnetic Laplacian for $g = 1/4$ and $g = 0$ (combinatorial), in the case of the Political Blogs network.

able to reveal both the directionality and connectivity patterns of the networks.

Acknowledgements

• EU: The research leading to these results has received funding from the European Research Council under the European Union's Seventh Framework Programme (FP7/2007-2013) / ERC AdG A-DATADRIVE-B (290923). This paper reflects only the authors' views, the Union is not liable for any use that may be made of the contained information. • Research Council KUL: GOA/10/09 MaNet, CoE PFV/10/002 (OPTEC), BIL12/11T; PhD/Postdoc grants. • Flemish Government: – FWO: G.0377.12 (Structured systems), G.088114N (Tensor based data similarity); PhD/Postdoc grants. – IWT: SBO POM (100031); PhD/Postdoc grants. • iMinds Medical Information Technologies SBO 2014. • Belgian Federal Science Policy Office: IUAP P7/19 (DYSCO, Dynamical systems, control and optimization, 2012-2017).

References

- [1] M. Belkin and P. Niyogi. Laplacian Eigenmaps for dimensionality reduction and data representation. *Neural Comput.*, 15(6):1373–1396, June 2003.
- [2] R. R. Coifman, S. Lafon, A. B. Lee, M. Maggioni, F. Warner, and S. Zucker. Geometric diffusions as a tool

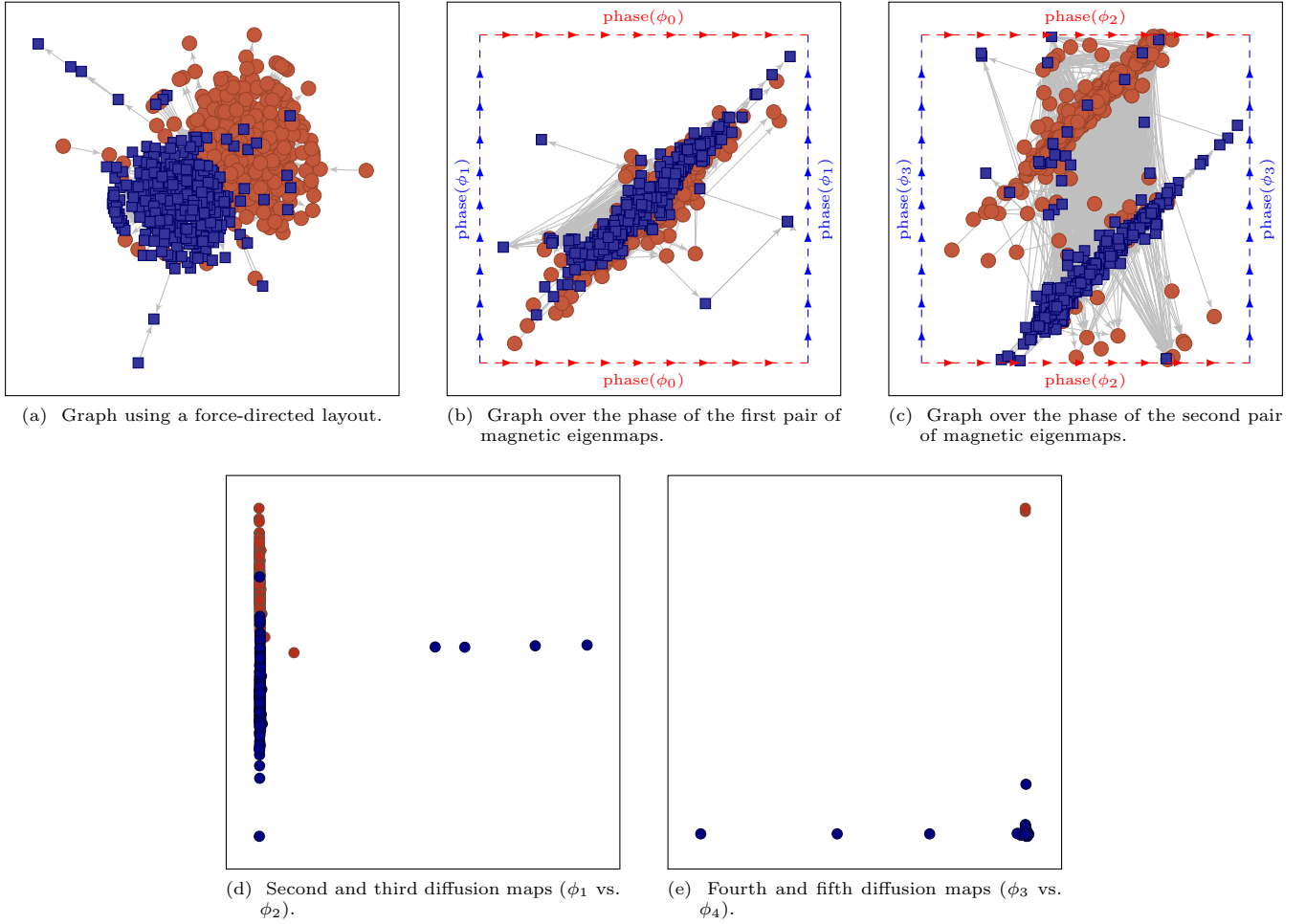


Figure 7: Political blogosphere example. The colours indicate the class labels: left leaning (●) and right leaning (●), and the magnetic eigenmaps correspond to $g = 1/4$. Figure 7c is shown in more detailed and also over the 3-dimensional torus in the SI appendix.

- for harmonic analysis and structure definition of data: Diffusion maps. In *Proceedings of the National Academy of Sciences*, pages 7426–7431, 2005.
- [3] D. C. Perrault-Joncas and M. Meila. Directed graph embedding: an algorithm based on continuous limits of laplacian-type operators. In *Advances in Neural Information Processing Systems*, pages 990–998, 2011.
- [4] F. Chung. Laplacians and the Cheeger inequality for directed graphs. *Annals of Combinatorics*, 9:1–19, 2005.
- [5] Q. Zheng and D. B. Skillicorn. Spectral embedding of directed networks. In *2015 IEEE/ACM International Conference on Advances in Social Networks Analysis and Mining (ASONAM)*, pages 432–439, 2015.
- [6] R. Kenyon. Spanning forests and the vector bundle Laplacian. *The Annals of Probability*, 39(5):1983–2017, 2011.
- [7] R. Forman. Determinants of Laplacians on graphs. *Topology*, 32(1):35–46, 1993.
- [8] M. Fanuel, C. M. Alaíz, and J. A. K. Suykens. Magnetic eigenmaps for community detection in directed networks. *ArXiv e-prints*, June 2016.
- [9] M. A. Shubin. Discrete magnetic Laplacian. *Comm. Math. Phys.*, 164:259–275, 1994.
- [10] Y. Colin de Verdière. Magnetic interpretation of the nodal defect on graphs. *Analysis and PDE*, 6(5):1235–1242, 2013.
- [11] G. Berkolaiko. Nodal count of graph eigenfunctions via magnetic perturbations. *Analysis and PDE*, 6(5):1213–1233, 2013.
- [12] A. Singer and H.T. Wu. Vector Diffusion Maps and the connection Laplacian. *Commun Pure Appl Math.*, 65(8):1067–1144, 2012.
- [13] X. Jiang, L.-H. Lim, Y. Yao, and Y. Ye. Statistical ranking and combinatorial Hodge theory. *Math. Program.*, 127(1):203–244, 2011.
- [14] A. Lancichinetti and S. Fortunato. Benchmarks for testing community detection algorithms on directed and weighted graphs with overlapping communities. *Phys. Rev. E*, 80:016118, 2009.
- [15] E. A. Leicht and M. E. J. Newman. Community structure in directed networks. *Phys. Rev. Lett.*, 100(118703), 2008.
- [16] M. E. J. Newman. Finding community structure in networks using the eigenvectors of matrices. *Phys. Rev. E*, 74:036104, 2006.
- [17] L.A. Adamic and N. Glance. The political blogosphere and the 2004 us election,. in *Proceedings of the WWW-2005 Workshop on the Weblogging Ecosystem*, 2005.

SI appendix

Magnetic Eigenmaps over torus

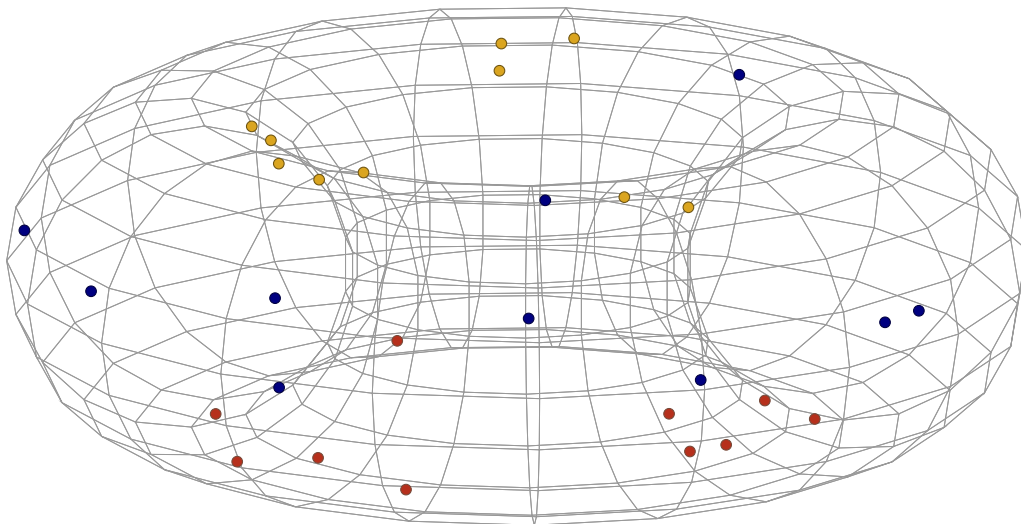


Figure S1: Phase of the magnetic eigenmaps plotted over the 3-dimensional 2-torus for the artificial network with a running flow (see Figure 3c).

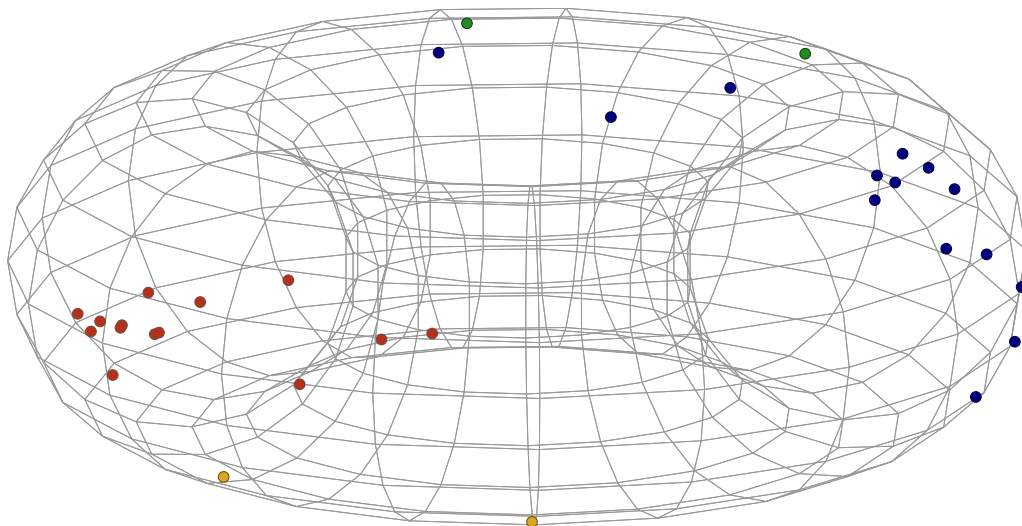


Figure S2: Phase of the magnetic eigenmaps plotted over the 3-dimensional 2-torus for the artificial network with two dense clusters and two pairs of nodes (see Figure 4c).

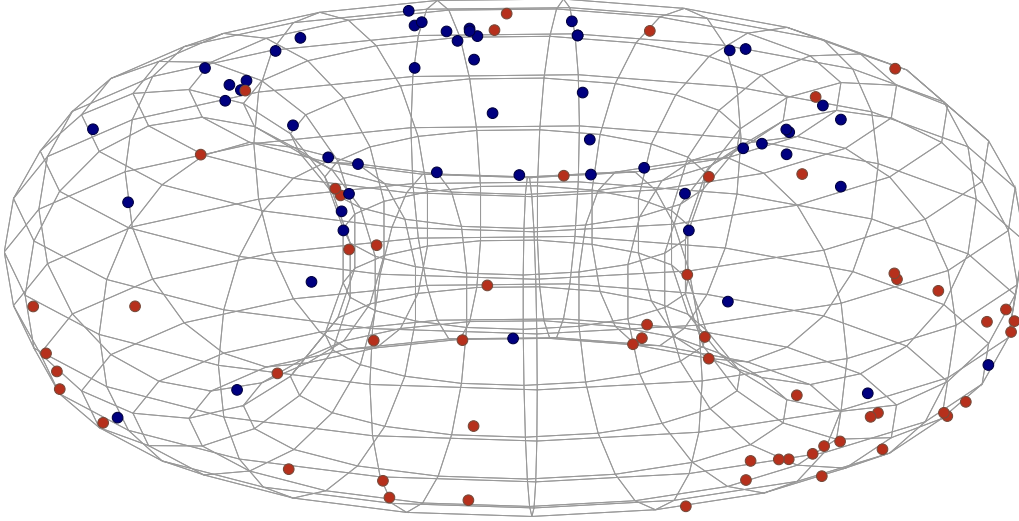


Figure S3: Phase of the magnetic eigenmaps plotted over the 3-dimensional 2-torus for the word adjacencies network (see Figure 5b).

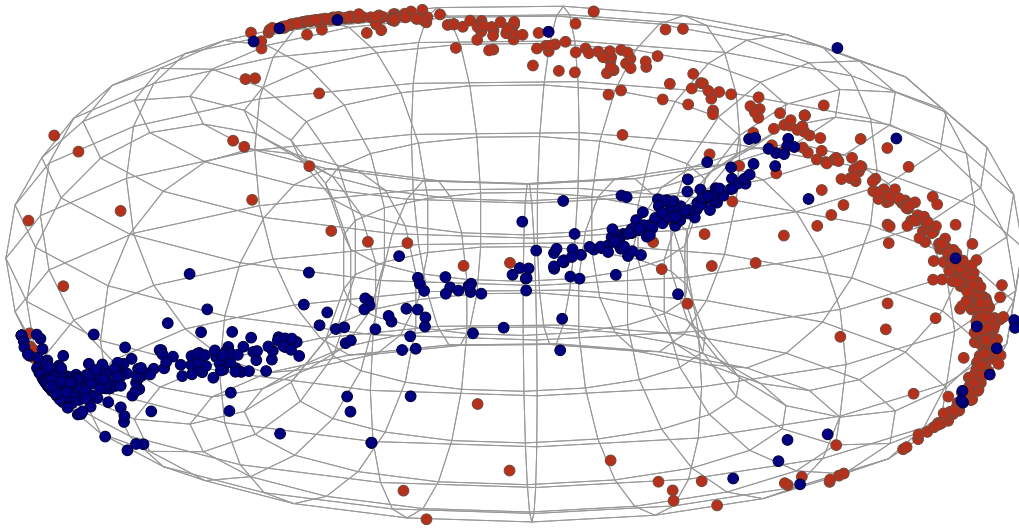


Figure S4: Phase of the magnetic eigenmaps plotted over the 3-dimensional 2-torus for the political blogosphere network (see Figure 7c).

